Anion Photoelectron Spectroscopy and Density Functional Investigation of Vanadium Carbide Clusters

K. L. Knappenberger, Jr.,[†] C. E. Jones, Jr.,[†] M. A. Sobhy,[†] I. Iordanov,[‡] J. Sofo,[‡] and A. W. Castleman, Jr.*[,†,‡]

Departments of Chemistry and Physics, The Pennsylvania State University, University Park, Pennsylvania 16802

Received: August 15, 2006; In Final Form: September 27, 2006

The influence of source conditions on vanadium−carbon cluster formation in a methane−vanadium plasma is explored and analyzed by photoelectron spectroscopy, revealing that the metal−carbon ratio has substantial influence over the cluster products. Experiments that employ large methane content produce carbon-rich mono- and divanadium carbides. The carbon-rich clusters show a preference for the formation of cyclic neutral and linear ionic structures. When the methane concentration is decreased, V_mC_n clusters are formed with $m = 1-4$ and $n = 2-8$. The photoelectron spectra of clusters formed under these conditions are indicative of a three-dimensional network. We have measured a significantly lower vertical electron affinity for the VC_2, V_2C_3, and V_4C_6 clusters compared with proximate species. Interestingly, the VC_2 species is a proposed building block of the M_8C_{12} Met-Car cluster, and the 2,3 and 4,6 clusters correspond to the 1/4 and 1/2 Met-Car cages, respectively. This correlation is taken as evidence of their importance in the formation of the larger Met-Car species. These results are supported by density functional theory (DFT) calculations carried out at the PBE/GGA level.

I. Introduction

Transition metal−carbon clusters exist in a variety of structural motifs that are highly dependent on the valence electronic configuration of the metal. Two specific classes of transition-metal carbon clusters include both metallocarbohedrenes[1] and metallofullerenes.[2] These species have been studied extensively in recent years with interest stemming from the cluster assemblies' ability to provide insight into the interaction between transition metals and carbon, significant not only to organometallic chemistry but to many areas of technological importance that include semiconductor science, hydrogen storage,[3] and catalysis.[4,5] In 1992, we reported the discovery of the former class of metal−carbon clusters mentioned above, metallocarbohedrenes or Met-Cars for short; the term metallocarbohydrynes now seems more in keeping with the latest structural calculations.[6] These clusters, with stoichiometry M_8C_{12}, where M is an early transition metal, show exceptional stability in the gas phase.[1,7] To date, Met-Cars have been formed from several metals that include Ti, V, Zr, Nb, Mo, Hf,[8−11] Cr,[11] Fe,[11] as well as in binary forms with molecular formula $Ti_{8-x}M_xC_{12}$ where M can be Si, Y, Zr, Nb, Mo, Hf, Ta, and W.[9,10]

The enhanced stability displayed by Met-Car clusters, as well as their facile formation by multiple metals, has stimulated a wealth of research. As a result, a great deal of information regarding the properties of Met-Cars has been gained, including trends in their ionization potentials[12] and electron affinities.[13] Met-Cars also exhibit significant delayed ionization when irradiated with nanosecond laser pulses[14,15] and display rapid electronic relaxation on ultrafast time scales.[16,17] Collectively, these findings suggest Met-Cars possess some degree of free electronic behavior. The unique electronic properties of Met-Cars, and other metal carbon clusters, render them as ideal candidates for many technological applications. Recently, density functional calculations by Muckerman and co-workers[4,5] have indicated that Met-Cars are likely to demonstrate enhanced catalytic properties that may enable them to be useful models for pollution abatement. Specifically, the results show that Ti_8C_{12}[4] and Mo_8C_{12}[5] have an activity for hydrodesulfurization that is greater than that of the presently employed molybdenum carbide catalysts. Recently, it has also been suggested that Met-Cars may be promising candidates for hydrogen storage applications.[3]

The successful implementation of Met-Cars and other cluster assembled materials necessitates a more complete understanding of the unique properties often displayed by matter of finite dimensions. This calls for more detailed information regarding the electronic and geometric structures of these clusters, and bulk-scale synthesis requires more insight regarding their growth processes. This has led us to address these questions from a bottom-up approach. Anion photoelectron spectroscopy has proved to be a powerful technique to understand the influence of evolving size on the electronic and geometric structure of cluster assemblies.[18] By measuring the photoelectron spectra of mass-selected gas-phase clusters, we can determine their properties on an individual basis and draw connections between species displaying similarities. This method has the advantage of enabling one to exercise environmental control over the cluster growth process while correlating these effects with the measured photoelectron spectra. In so doing, this approach enables a direct determination of how the cluster's properties may be tailored. The MC_2 unit has been proposed to serve as the building block from which the larger three-dimensional (3D) Met-Car clusters are formed.[1,19] Previous experiments have suggested that the VC_2 cluster is likely to be important to the

* To whom correspondence should be addressed. E-mail: AWC@psu.edu.
[†] Department of Chemistry, The Pennsylvania State University.
[‡] Department of Physics, The Pennsylvania State University.

10.1021/jp065273g CCC: $33.50
Published on Web 11/09/2006

formation of a larger metal−carbide network.[20−22] However, little information is available for cluster sizes that extend beyond V_2C_4, and a gap exists in the understanding of the properties of clusters up to the V_8C_{12} Met-Car. In this contribution, we present data that extends the existing literature to include larger metal−carbide clusters consisting of as many as four metal atoms. Additionally, we have explored the influence of source conditions on the resultant cluster products. Comparisons are made with recent studies of niobium−carbon clusters,[23] which display interesting geometric properties that are strongly influenced by cluster source conditions.

II. Experimental Section

A detailed description of the experimental apparatus is the primary focus of a separate report,[24] and as such, only a brief overview will be provided here. Vanadium carbide clusters are generated in a 10 Hz laser vaporization plasma reactor source in which the second harmonic (532 nm) of a Nd:YAG laser is focused on a translating and rotating vanadium rod, forming a plasma. Typically, a helium carrier gas is seeded with 5% methane and passed over the plasma, leading to the dehydrogenation of methane and the formation of metal carbide clusters. In this study, we have also investigated the formation of vanadium carbide clusters in a carbon-rich environment where the methane content of the carrier gas exceeds 10%. The anions are subsequently pulse extracted, and the cluster distribution is analyzed by a linear time-of-flight mass spectrometer. The resolution ($m/\Delta m$) of the mass spectrometer is currently greater than 750, which is more than sufficient for the cluster sizes studied here. The cluster of interest is then mass selected prior to photodetachment. Following mass selection, electrons are detached with the third harmonic of a Nd:YAG (355 nm, 3.49 eV) or with a XeCl Excimer laser (308 nm, 3.02 eV). Detached electrons are collected by a "magnetic bottle" type photoelectron spectrometer, where a strong (1.2 T) permanent magnet is used to collect electrons over approximately 4π radians.[24,25] The detached electrons traverse a low field (10^{-3}T) drift region before detection by a Z-stack microchannel plate (MCP) detector. The measured ion current from the MCP is then amplified before collection by a digital oscilloscope and is transferred through a GPIB card to a PC for analysis. The magnetic bottle electron kinetic energy analyzer is calibrated daily by photodetachment of Cu^-. The known photodetachment spectrum[26] of Cu^- includes transition from the Cu^- ground state ($^1S_0$, $3d^{10}4s^2$) to the Cu ground state ($^2S_{1/2}$, $3d^{10}$ $4s^1$) as well as the first two Cu excited states ($^2S_{5/2}$, $3d^9 4s^2$) and ($^2S_{3/2}$, $3d^9$-$4s^2$). The electron kinetic energy resolution of the experiments is better than 140 meV at 1.2 eV, as determined by fitting a Gaussian function to the atomic copper transition. The experimental findings were verified computationally with density functional theory (DFT) at the PBE level using the GGA/PBE exchange[27,28] using the DMol3 program.[28] The basis set is a double numerical basis set with polarization functions provided by the Dmol3 code. It uses an orbital cutoff of 5 Å. All the calculations are spin unrestricted and smearing is not used, nor is there special treatment of the core electrons.

III. Results and Discussion

The mass distribution shown in Figure 1A represents the anionic clusters generated in the laser vaporization source with low methane content (<5% CH_4/He). This is the source condition that is found to be favorable for the generation of larger metal−carbide clusters including Met-Cars. Indeed, we have formed larger clusters with greater M/C ratios than reported here by systematically varying the source conditions, and these studies are ongoing. The mass distribution indicates that $V_mC_n^-$ clusters, where $m = 1-4$, are readily formed under the conditions employed. The cluster distribution shown in Figure 1B is obtained by increasing the methane content to 10% or greater. As can be seen in the mass distribution, these conditions lead to the formation of primarily high carbon clusters containing only a few vanadium atoms. In fact, clusters containing more than two metal atoms are not generated under these conditions. The distribution is dominated by $V_mC_n^-$ where when $m = 1$, $n = 2-6$ and when $m = 2$, $n = 3-12$. We have demonstrated clean mass selection of clusters in this size range.[24]

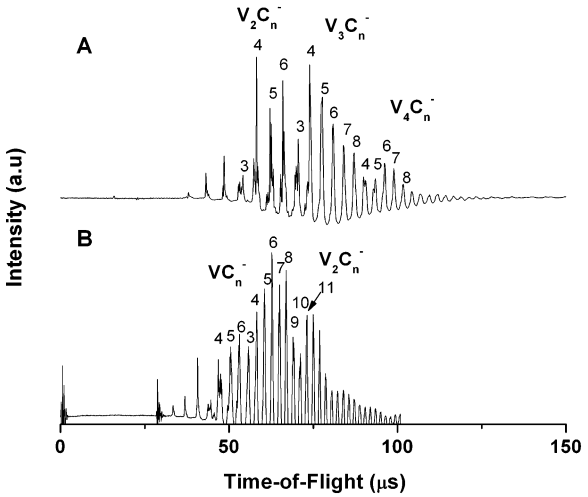

Figure 1. Time-of-flight mass distributions of clusters formed with low (A) and high (B) concentrations of methane.

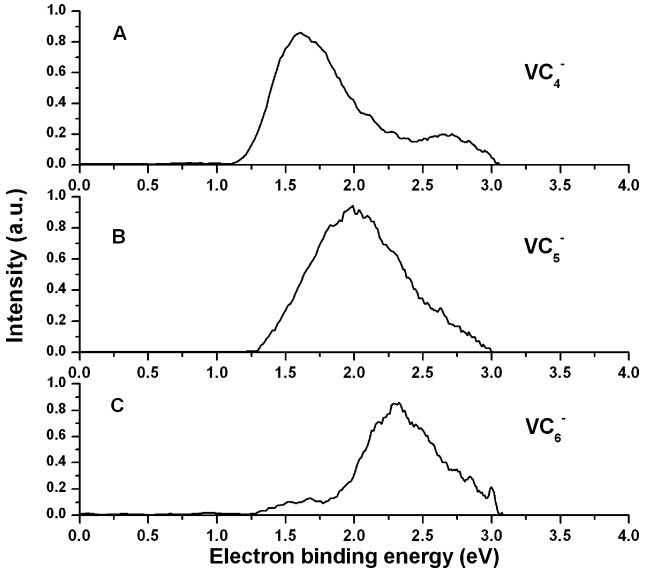

Figure 2. Photodetachment spectra of VC_4^-, VC_5^-, and VC_6^-.

III.A. Monovanadium Carbides. The electron kinetic energy distribution for monovanadium carbides, generated with high carbon content, is shown in Figure 2, and all electron binding energies measured are reported in Table 1. The photoelectron energy spectrum of VC_4^- is shown in Figure 2A and displays a dominant feature with a measured vertical electron affinity of 1.3 eV and a second, less intense, feature shifted to a higher binding energy of 2.5 eV. The vertical electron affinity is determined by the common method[20] of fitting a linear function to the leading edge of each energy shift and setting the *y*-intercept as the binding energy. This method provides the vertical electron detachment energy of the cluster and thereby

TABLE 1: Measured Electron Binding Energies[a]

low carbon content		high carbon content	
cluster	binding energy (eV)	cluster	binding energy (eV)
		VC_4	X 1.2
			A 2.5
		VC5	X 1.4
		VC_6	X 1.3
			A 1.8
V_2C_3	X 1.5	V_2C_7	X 1.7
V_2C_4	X 1.9	V_2C_8	X 2.4
V_2C_5	X 1.8	V_2C_9	X 1.8
	A 3.0	V_2C_{10}	X 1.4
V_2C_6	X 1.7	V_2C_{11}	X 1.5
	A 2.8		
V_3C_3	X 1.7		
V_3C_4	X 1.9		
V_3C_5	X 1.8		
V_3C_6	X 1.6		
V_4C_4	X 1.7		
V_4C_5	X 1.7		
V_4C_6	X 1.4		
V_4C_7	X 1.7		

[a] Reported values are obtained from the measured vertical detachment energy. The uncertainty of the measurements is ± 0.14 eV.

provides information on the vertical electron affinity (VEA). The photoelectron spectra of VC_5^- and VC_6^- are displayed in parts B and C of Figure 2, respectively. The vertical electron affinity of VC_5 is determined to be 1.4 eV. The most intense feature in the VC_6 photodetachment spectrum is located at 1.7 eV and interestingly is not the lowest energy feature. A feature appears with much lower intensity at a binding energy of 1.3 eV, and this value is taken as the vertical electron affinity of VC_6. The measured vertical electron affinities of the monovanadium carbides studied here, as well as values obtained from previous studies,[29,30] are summarized schematically in Figure 7A, which will be discussed later. It is interesting to note the even−odd alternation that develops with cluster size. This pattern is reminiscent of pure carbon[31,32] or carbon-rich metal−carbide clusters.[23,33,34] This alternation is typically accepted as a sign of linear geometry when the alternation between even and odd cluster sizes is very strong. The alternation observed here, on the other hand, is rather weak and the determined vertical electron affinities are much lower than those typically associated with linear structures. Moreover, the measured electron affinity does not change dramatically with increasing cluster size. These findings are similar to those reported previously for monotitanium carbides[34] and our findings on diniobium carbide clusters.[23]

Pure carbon clusters in the size range considered here are known to have high electron affinities, easily exceeding 2 eV.[31] The low electron affinities measured for the monovanadium carbides is an indication that the highest occupied molecular orbital (HOMO) of these clusters is likely attributed to the contribution of a vanadium 3d orbital. This is reasoned since the electron affinity of a gas-phase vanadium atom has been assigned as 0.525 eV,[36] much lower than that of carbon clusters. The fact that increasing the number of carbon atoms has little influence over the electron affinity of the monovandium series indicates that there is little alteration of the bonding environment of the vanadium atom, where the excess electron likely resides. Previous results that measured the photoelectron spectra of VC_2[29] and VC_3[30] concluded that a planar structure of C_{2v} symmetry was formed for both. We have reproduced these experimental measurements and find agreement with the previously reported values. Additionally, we have treated several anionic and neutral cluster sizes computationally at the B3LYP and PBE levels of DFT. As will be discussed, the results from the PBE level provide the best fit to the experimental data, and the stable anionic geometric structures obtained from this method are summarized in Figure 3 along with the computed energy difference (ΔE) relative to the minimum energy structure, adiabatic electron affinity (AEA), and vertical electron affinity (VEA). The calculated energy difference between the linear $C_{\infty v}$ and the triangular C_{2v} structure of VC_2 is approximately 0.156 eV, indicating that the linear chain is the most stable anionic geometry. However, calculations carried out at the same level for the neutral show that the C_{2v} geometry is more stable than the linear $C_{\infty v}$ isomer by 0.874 eV. The small change in electron affinity in the range of clusters between VC_2 and VC_6 (Table 1) is taken as a sign of the continuation of geometric structure for the monovanadium carbon clusters.

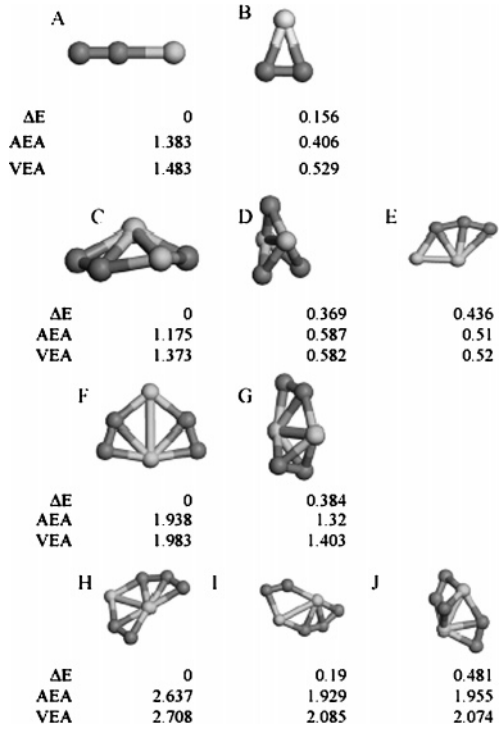

Figure 3. Calculated geometric structure for several V_mC_n clusters carried out at the PBE/GGA level of density functional theory. The energy difference between the clusters, relative to the minimum energy structure, is reported along with the adiabatic electron affinity (AEA) and the vertical electron affinity (VEA) for each size. The computational results are for cluster sizes VC_2 (A−B), V_2C_3 (C−E), V_2C_4 (F−G), and V_2C_5 (H−J).

In complementary work from our group,[23] direct experimental evidence was found for the coexistence of structural isomers of diniobium carbides. The electron energy spectra of these clusters are comprised of two distinct peaks. The first peak appears in the binding energy range of 1.2−1.7 eV while the second peak appears in the binding energy range between 2.2 and 3.0 eV. The high and low binding energy features are likely to originate from linear and cyclic isomers, respectively. These findings are consistent with measurements found in the existing literature regarding high carbon−metal clusters.[30−32] The low electron affinities reported here, taken together with the small influence of cluster size effects, lead us to conclude that these monovanadium clusters are likely of a common geometry. The DFT results suggest that the lowest energy structure for the anion is linear, however, calculations carried out at the same level for neutral species indicate that the triangular structure (C_{2v}) is the most stable isomer.

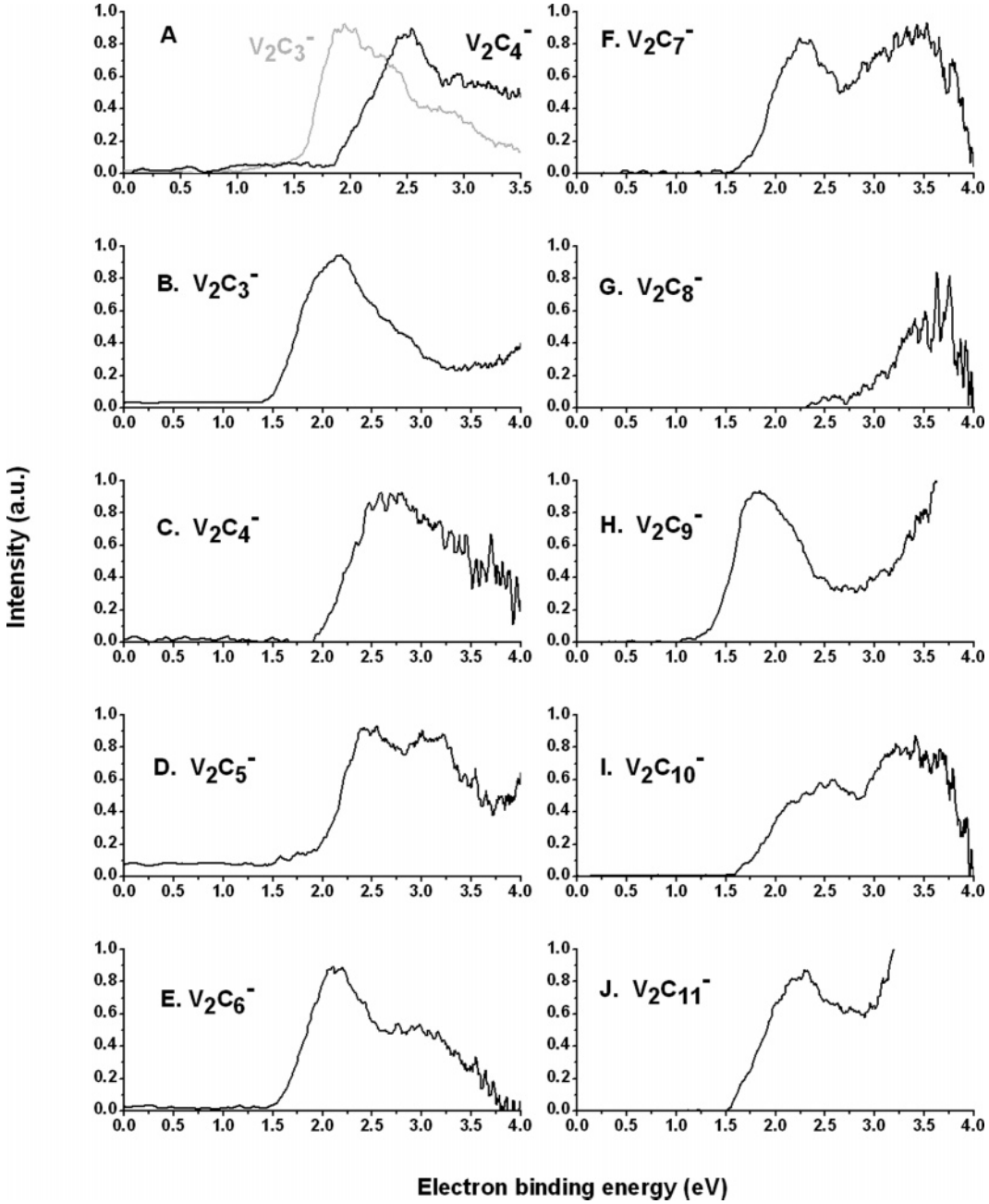

Figure 4. Photodetachment spectra of V_2C_n clusters formed with source conditions of low (left) and high (right) methane content.

III.B Divanadium Carbides. The photodetachment spectra of divanadium carbon clusters are shown in Figure 4. The photodetachment spectra presented on the left panel are obtained from clusters generated with $\leq$5% methane seeded in helium carrier gas. The high carbon species shown in the right panel of Figure 4 are formed with $\geq$10% methane in helium. We note that, while data on the Met-Car is not presented here, the former source condition is closest to the one preferential to formation of larger, metal-enriched clusters such as Met-Cars. In panel A of Figure 4, a comparison of the electron energy spectra of $V_2C_3^-$ and $V_2C_4^-$ obtained at 355 nm, the third harmonic of a Nd:YAG laser, is shown. The spectra presented in the remaining panels of Figure 4 are obtained by photodetachement with a 308 nm XeCl Excimer laser. The electron energy spectra of $V_2C_3^-$ and $V_2C_4^-$ are presented individually in panels B and C of Figure 4, respectively. The vertical electron affinity determined for V_2C_3 is 1.5 eV, and a significant increase is observed in going to V_2C_4, which has a measured vertical electron affinity of 1.9 eV. These measurements are in excellent agreement with the values reported for the vertical electron affinities of V_2C_3 and V_2C_4 previously.[20,21] The remainder of the divanadium carbon clusters formed with the source conditions of lower methane content are shown in panels D and E of Figure 4 and are plotted schematically in Figure 7B, as discussed in later sections. The electron energy spectra of V_2C_5 and V_2C_6 each reveal the presence of an additional feature with binding energy greater than 2.5 eV (refer to Table 1). The origin of these features could be due to the coexistence of multiple isomeric forms or a photodetachment to a neutral excited state. Further experiments and theoretical studies may be necessary to properly assign these features, but our computational results presented here provide evidence for the former case. It is interesting to note that there is a significant increase in electron affinity in going from V_2C_3 to V_2C_4. Moreover, while there is a decrease in the electron affinity from V_2C_4 to V_2C_5 and again from V_2C_5

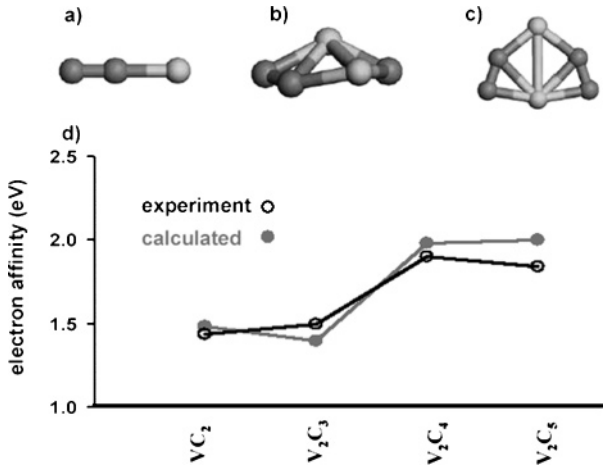

Figure 5. Geometric structure of the (a) VC_2, (b) V_2C_3, and (c) V_2C_4 clusters. (d) Comparison of calculated and measured vertical electron affinities of selected V_mC_n clusters. Results obtained from density functional calculations at the PBE/ GGA level.

to V_2C_6, the V_2C_3 cluster has the lowest measured electron affinity of those presented in the left panel of Figure 4.

Computation of the geometric structures giving rise to the experimentally measured trends in photodetachment spectra for these cluster sizes has been carried out. We have considered many different geometries of the VC_2 and V_2C_n clusters (with $n = 3-5$). The calculated vertical electron affinities of structures based on the build-up from VC_2 units exhibit trends that best track with the experimental data. This trend is shown in Figure 5. The geometric isomers for VC_2, V_2C_3, and V_2C_4 that best reproduce the experimental observations are presented in panels A−C of Figure 5, respectively. In Figure 5D, we compare the vertical electron affinities that we measure experimentally with those calculated based on the structures presented in panels A−C of Figure 5. It should be noted that the computational electron affinities were determined at multiple levels of DFT, but as is clear in Figure 5D the PBE level provides an excellent match to experimental measurements. The comparison made in Figure 5D is made without shifting the computational results. The trend in both the calculated and experimental measurements is the important aspect, showing an increase in electron affinity in going from V_2C_3 to V_2C_4. The overlay of the computational and experimental results shows that the values track well with one another and verify our assignment of the structures presented in panels A−C of Figure 5, suggestive of the replication of VC_2 in the cluster growth process. The geometric structures of V_2C_3 and V_2C_4 have been computed previously and are in general agreement with our results.[22] In fact, we find nearly identical structures for the V_2C_4 cluster; however, we find that the structure presented in Figure 5B better matches our experimental observations than that previously reported for V_2C_3. The formerly reported structure of V_2C_3 was a planar cycle consisting of a vanadium dimer that joined the carbon atoms. We find the V_2C_3 cluster is stabilized when the carbon atoms bend out of the plane of the V_2 unit. This cluster size likely marks the onset of 3D structure. The computational results indicate the 3D structure of $V_2C_3^-$ in Figure 3C is of lower energy than the other structures (in parts D and E of Figure 3) by at least 0.369 eV. Furthermore, the calculated difference in vertical electron affinity of the structure in Figure 3C and those in parts D and E of Figure 3 is on the order of 750 meV. The experimental resolution of these studies is 150 meV, and therefore, the presence of other geometric isomers of V_2C_3 in the molecular beam can be ruled out. It is also interesting to note that structures not containing the VC_2 unit are not found to be stable by the DFT calculatons.

We find that the VC_2, V_2C_3, and V_2C_4 clusters that match our experimental findings also correspond to the lowest computed energy structure for the cluster size. However, this is not the case for the V_2C_5 cluster. In fact, there are two isomers of V_2C_5 separated by 0.19 eV (structures H and I in Figure 3), and their calculated electron affinities do coincide with the experimental trends. The measured binding energies of the two peaks in Figure 4D are 1.8 and 3.0 eV, refer also to Table 1. The vertical electron affinities determined at the PBE level for structures H and I in Figure 3 are 2.708 and 2.085 eV, respectively. The high temperature of the plasma reactor likely leads to a distribution of accessible cluster geometries, thereby enabling the higher energy structure for V_2C_5 to be formed. The lowest energy structure of V_2C_5 (Figure 3H) is similar to the lowest energy structure for V_2C_4 (Figure 3F) and strongly resembles the most recent computational work of the Met-Car cluster.[6] The two experimentally measured photoelectron peaks are assigned to isomers H and I in Figure 3.

The detachment spectra of clusters presented in the right panel of Figure 4 are from clusters formed under conditions of higher carbon content. The detachment spectra of V_2C_7 through V_2C_{11} are presented in panels F−J of Figure 4, respectively. The vertical electron affinities are also mapped out schematically in Figure 7B (to be discussed later). As is evident from the photodetachment data in Figure 4 and the summary plot of Figure 7B, an even−odd alternation exists for the high carbon clusters similar to that observed for the monovanadium carbon series. The largest alternation is observed in going from the V_2C_8 to the V_2C_9 cluster. On average, the alternation observed in this series is small and the measured energies fall in the range typically associated with planar ring structures. A high binding energy feature is measured in the detachment spectra for V_2C_7 and V_2C_{10} clusters. These peaks could be attributed to an alternative isomeric structure or an excited electronic state. Currently, we are pursuing this issue with both experimental and computational methods. It is important to note, however, that a transition from the low-energy feature to the high-energy feature as the dominant species is never observed. The photodetachment experiments reported for the diniobium carbon cluster showed a transition to linear structure in going from the Nb_2C_6 to the Nb_2C_7 and a likely transition back to a cyclic structure when nine carbon clusters were incorporated.[23]

It is surprising at first to find that the niobium clusters show a clear transition to linear geometry and that this is not reproduced in the divanadium series since both are group V metals. A likely important difference is in the valence electronic configuration of the two metals. Niobium is the first group V metal that promotes an s electron to a d orbital, resulting in a $5s^14d^4$ valence electronic configuration. This promotion leaves niobium with four d valence electrons that can undergo hybridization and bond similarly to carbon, as well as allowing the s-orbital to remain open for bonding. Vanadium on the other hand does not promote an s electron resulting in a $4s^23d^2$ configuration. This leaves vanadium with a filled s orbital that is unable to participate in the covalent interactions that we have found to be important to the formation of the niobium carbon clusters.[23] As a consequence, an important difference between the two types of clusters is likely rooted in the bond strength of the metal−metal and metal−carbon interactions dictated by the metals electronic configuration. Results from DFT indicate that the V_2C_2 cluster retains strong V−V bonding attributed to the high dissociation energy of the vanadium dimer (2.75 eV).[21]

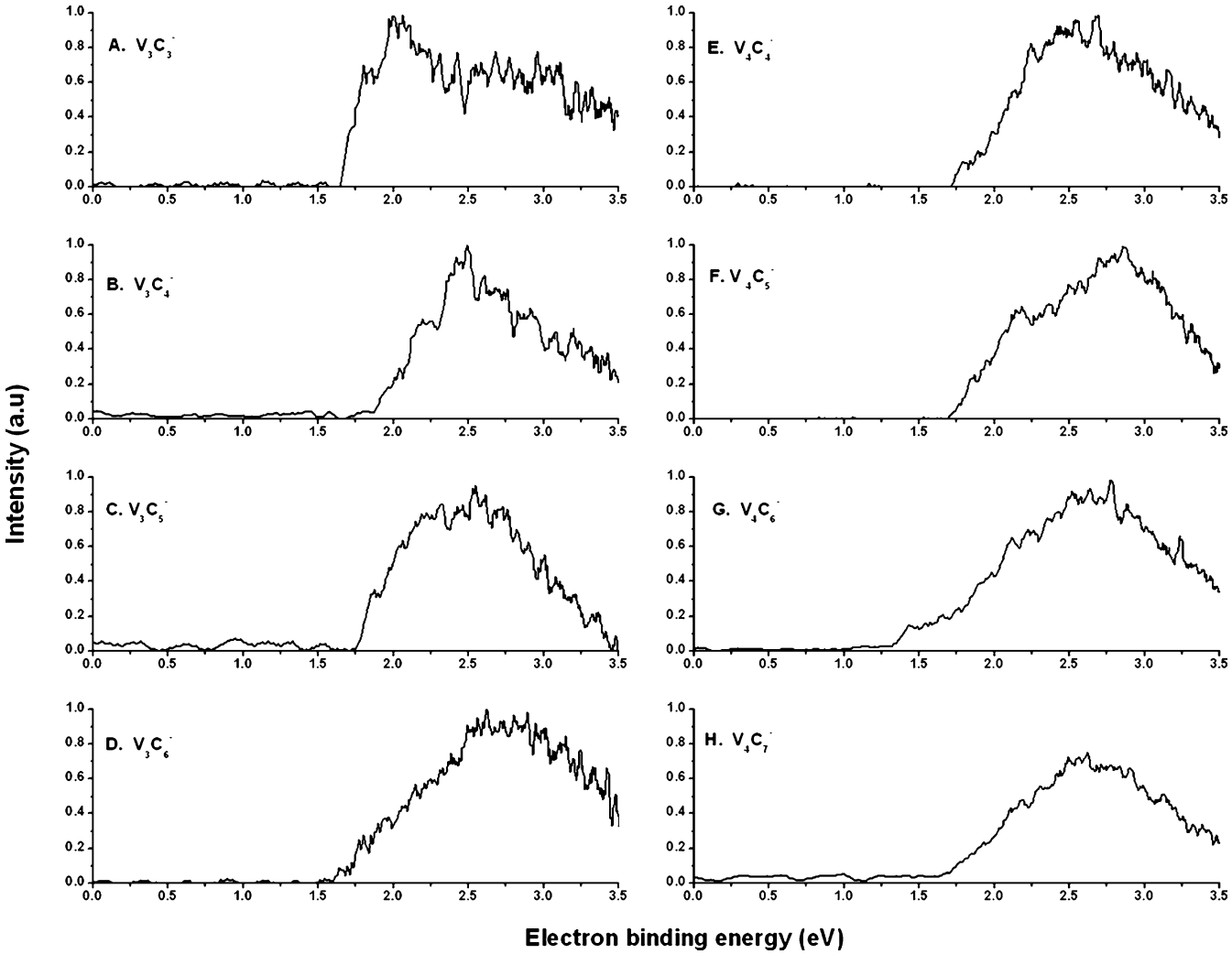

Figure 6. Anion photodetachment spectra of $V_3C_n^-$ (left) and $V_4C_n^-$ (right). All V_3 and V_4 clusters studied were formed under source conditions with low methane content.

Conversely for the Nb_2C_2 cluster, the niobium dimer has been found to dissociate without barrier[37] and these results suggest that niobium−carbon bonds are much more stabilizing than metal−metal interactions.

The findings on niobium−carbon clusters are the subject of a separate report.[23] The observation that niobium readily alternates between bonding types that form both linear and cyclic isomers is likely to result from an overlap of a carbon molecular σ-orbital with an atomic niobium s orbital. This is perhaps one reason for the experimental observation of coexisting isomers for niobium, while such structures are not observed for vanadium. This suggests that larger carbon-rich vanadium clusters should prefer a cyclic structure that retains the vanadium−vanadium interaction. Since preservation of the V−V moiety is stabilizing, it may help to overcome ring-strain that would likely be induced in larger cyclic structures. The anionic linear structure for vanadium carbides may be the result of an ion pair that is formed between the stable carbon chain and the vanadium atom, which retains the excess electron, when high carbon source conditions are employed. Typically, contact ion pairs are size dependent, and when one member of the pair becomes large relative to the other, the ion pair is no longer stable. Alternatively, the open s orbital on the niobium atom would be available for covalent bonding with carbon, leading to the formation of large metal−carbon networks in high carbon clusters. In referring to the mass spectra in Figure 1, it is true that the vanadium cluster distribution truncates at relatively small cluster sizes when high carbon source conditions are employed, as in Figure 1B. When the same source conditions are employed with niobium, large clusters can be formed.

III.C Larger Vanadium Carbides: V_3 and V_4 Series Carbides. The photodetachment spectra of V_3 and V_4 series carbides are shown in the left and right columns of Figure 6, respectively. All V_3 and V_4 series clusters reported here were generated with lower levels of methane in the carrier gas (<5% CH_4/He). The cluster intensities of the V_3 and V_4 series were slightly less than those for the V_1 and V_2 series, so the third harmonic of the Nd:YAG (355 nm) was used for the larger clusters as it provides lower levels of background noise, slightly better photon densities, and a more defined beam profile. As is evident in both Figures 6 and 7C the lowest vertical electron affinity measured in the V_3 series is attributed to V_3C_3 and V_3C_6, which have comparable values. The electron affinity increases in going from V_3C_3 to V_3C_4, shown in Figure 6B, and then decreases in going to V_3C_4 to V_3C_6, similar to the trend observed for the V_2 series generated with lean methane concentrations.

The detachment results obtained from the V_4C_n series are shown in panels E−H of Figure 6. The vertical electron affinities are reported schematically in Figure 7C and numerically in Table 1. These results indicate that the lowest electron affinity in the V_4 series is attributed to the V_4C_6 cluster, an indication of enhanced stability of the neutral state. It should be noted that a

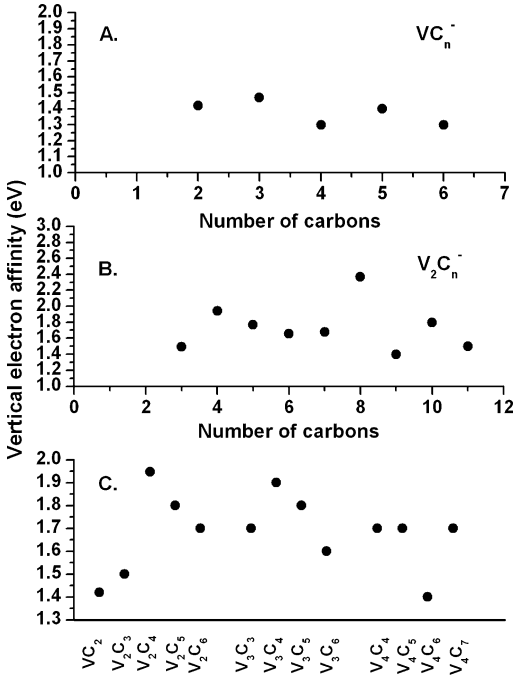

Figure 7. (A) Plot of electron affinity as a function of cluster size for the VC_n series. The values for VC_2 and VC_3 are from refs 19 and 20, respectively. (B) Plot of electron affinity as a function of cluster size for the V_2C_n series. (C) Plot of vertical electron affinity for all clusters formed with low methane source conditions.

cluster that is especially stable in the cationic state would display similar behavior. The V_4C_6 also appears to be unique when compared with the other cluster sizes. In addition to having the lowest electron affinity of the series, the V_4C_6 species also exhibits the broadest distribution of electron kinetic energies. This broad distribution is especially apparent at high electron binding energy, which corresponds to low kinetic energy electrons in the detachment experiment. Observation of broad electron kinetic energy distributions often reflects a geometric rearrangement in going from anionic to neutral potential surfaces. Measurement of broad energy distributions in photoelectron spectra also signifies the onset of thermalization processes that compete with direct emission. In accordance with the Richardson−Dushman equation,[38] the rate of indirect electron emission, resulting from thermalization, increases exponentially with decreasing work function (*W*, the bulk analogue of electron affinity).[39] The fact that the V_4C_6 species has the lowest electron affinity of the V_4 series may help to mediate indirect processes and be responsible for the broad distribution of electron affinities.

III.D General Considerations. Previous studies have indicated that the M_8C_{12} cluster has a significantly lower electron affinity than other cluster sizes in the distribution.[13] These findings, along with work from our group that showed exceptionally low ionization potentials for the neutral Met-Cars,[12] point to their enhanced stability in cationic forms. It is interesting to note that when referring to the electron affinity plot for all cluster sizes shown in Figure 7C that the clusters with the lowest electron affinities are the VC_2, V_2C_3, and V_4C_6 clusters. It has been a long standing belief that the MC_2 unit plays a significant role in the formation of Met-Car clusters, and recent work including the calculations and measurements reported here support this idea. Further, as demonstrated in this study, the other clusters which exhibit exceptionally low electron affinities are V_2C_3 and V_4C_6, which correspond to the 1/4 and 1/2 cage of the Met-Car. The low electron affinities of these clusters indicates that the nature of the HOMO is likely more similar to that of vanadium as carbon has a rather high electron affinity. While more detailed studies are needed for confirmation, it is likely that the HOMO of these clusters is significantly influenced by a vanadium 3d orbital. Previous work from our group has also revealed that the neutral Met-Car clusters undergo indirect processes, such as delayed electron emission.[14,15,40] The connection between the low electron affinities of the smaller subdivisions of Met-Cars and the M_8C_{12} cluster may be an indication that the broad electron energy distribution observed for V_4C_6 is due to indirect processes. The data provide indirect evidence that the MC_2 and 1/4 and 1/2 cage species do indeed play an important role in the formation of larger 3D clusters including the Met-Car. It is also noted that the cluster source conditions are highly influential over the types of cluster that are formed. We find that the presence of large amounts of methane in the source favor formation of high carbon species that incorporate only a few metal atoms. By decreasing the methane concentration, conditions that favor formation of larger 3D metal carbide clusters are found. These findings agree with earlier work on the formation of vanadium and titanium carbide clusters, which suggest that small differences in the metal−carbon densities can influence the clusters products that are formed.

IV. Conclusions

We have employed a range of cluster source conditions which have enabled us to investigate the photoelectron spectra of several vanadium carbon clusters. The structures of these clusters are likely neutral planar cyclic rings, anionic linear chains, and larger 3D clusters. We have found that the methane content of the cluster source influences these geometries significantly. Our results indicate that high carbon monovanadium cluster anions prefer a linear geometry, while the neutral species are most stable as planar cyclic rings. When going to the divanadium distribution, evidence exists for the transition to planar cyclic structures when the carbon content is high. Photodetachment experiments conducted on vanadium carbide clusters when the methane content is low indicate that the VC_2, V_2C_3, and V_4C_6 clusters exhibit the lowest electron affinity of the distribution. A lowering in electron affinity has also been reported previously for M_8C_{12} clusters. This is taken as evidence for the importance of VC_2, V_2C_3, and V_4C_6 in the formation of larger 3D clusters that include the Met-Car cluster. These findings are supported by computational results from DFT. Taken together, the experimental and computational findings reflect that the VC_2 unit serves as a precursor in the growth of large metal−carbon clusters. Comparisons with our recent complementary study on niobium−carbon clusters have also been made, and a fundamental picture has been suggested to explain the differing growth processes of the two metals.

Acknowledgment. The authors gratefully acknowledge funding from the U.S. Department of Energy, Building Blocks, Grant No. DE-FG02-02ER46009. One of the authors (A.W.C.) acknowledges valuable conversations with S. N. Khanna of Virginia Commonwealth University.

References and Notes

(1) Guo, B. C.; Kerns, K. P.; Castleman, A. W., Jr. *Science* **1992**, *255*, 1411.

(2) Clemmer, D. E.; Hunter, J. M.; Shelimov, K. B.; Jarrold, M. F. *Nature* **1994**, *372*, 248.

(3) Zhao, Y.; Dillon, A. C.; Kim, Y. H.; Heben, M. J.; Zhang, S. B. *Preprints of Symposia-American Chemical Society, Division of Fuel Chemistry* **2005**, *50*, 452.

(4) Lui, P.; Rodriguez, J. A.; Muckerman, J. T. *J. Phys. Chem. B* **2004**, *108*, 15662.
(5) Lui, P.; Rodriguez, J. A.; Muckerman, J. T. *J. Phys. Chem. B* **2004**, *108*, 18796.
(6) Sobhy, M. A.; Castleman, A. W., Jr.; Sofo, J. O. *J. Chem. Phys.* **2005**, *123*, 154106.
(7) Guo, B. C.; Wei, S.; Purnell, J.; Buzza, S.; Castleman, A. W., Jr. *Science* **1992**, *256*, 515.
(8) Cartier, S. F.; May, B. D.; Castleman, A. W., Jr. *J. Chem. Phys.* **1994**, *100*, 5384.
(9) Cartier, S. F.; May, B. D.; Castleman, A. W., Jr. *J. Am. Chem. Soc.* **1994**, *116*, 5295.
(10) Leskiw, B. D.; Castleman, A. W., Jr. *C. R. Phys.* **2003**, *3*, 251.
(11) Pilgrim, J. S.; Duncan, M. A. *J. Am. Chem. Soc.* **1993**, *115*, 9724.
(12) Sakurai, H.; Castleman, A. W., Jr. *J. Phys. Chem. A* **1998**, *102*, 10486.
(13) Wang, L. S.; Li, S.; Wu, H. *J. Phys. Chem.* **1996**, *100*, 19211.
(14) May, B. D.; Cartier, S. F.; Castleman, A. W., Jr. *Chem. Phys. Lett.* **1995**, *242*, 265.
(15) Kooi, S. E.; Castleman, A. W., Jr. *J. Chem. Phys.* ***1998***, *108*, 8864.
(16) Kooi, S. E.; Leskiw, B. D.; Castleman, A. W., Jr. *Nano Lett.* **2001**, *1*, 113.
(17) Leskiw, B. D.; Knappenberger, K. L.; Castleman, A. W., Jr. *J. Chem. Phys.* **2002**, *117*, 8321.
(18) Stolow, A.; Bragg, A. E.; Neumark, D. M. *Chem. Rev.* **2004**, *104*, 1719.
(19) Wei, S.; Guo, B. C.; Purnell, J.; Buzza, S.; Castleman, A. W., Jr. *J. Phys. Chem.* **1992**, *96*, 4166.
(20) Tono, K.; Teraski, A.; Ohta, T.; Kondow, T. *Chem. Phys. Lett.* **2002**, *351*, 135.
(21) Tono, K.; Teraski, A.; Ohta, T.; Kondow, T. *J. Chem. Phys.* **2002**, *117*, 7010.
(22) Rohmer, M. M.; Benard, M.; Poblet, J. *Chem. Rev.* **100**, 495 **2000**.
(23) Knappenberger, K. L., Jr.; Sobhy, M. A.; Jones, C. E., Jr.; Sofo, J.; Castleman, A. W., Jr. Manuscript in preparation.
(24) Knappenberger, K. L., Jr.; Jones, C. E., Jr.; Sobhy, M. A.; Castleman, A. W., Jr. *Rev. Sci. Instrum.*, submitted for publication.
(25) Kruit, P.; Read, F. H. *J. Phys. E* **1983**, *16*, 313.
(26) Wang, L. S.; Cheng, H. S.; Fan, J. *J. Chem. Phys.* **1995**, *102*, 9480.
(27) Perdew, J. P.; Burke, K.; Ernzerhof, M. *Phys. Rev. Lett.* **1996**, *77*, 3865.
(28) Delley, B. *J. Chem. Phys.* **1990**, *92*, 508.
(29) Li, X.; Wang, L. S. *J. Chem. Phys.* **1999**, *111*, 8389.
(30) Wang, L. S.; Li, X. *J. Chem. Phys.* **2000**, *112*, 3602.
(31) Yang, S.; Taylor, K. J.; Craycraft, M. J.; Conceicao, J.; Pettiette, C. L.; Cheshnovsky, O.; Smalley, R. E. *Chem. Phys. Lett.* **1988**, *114*, 431.
(32) Arnold, D. W.; Bradforth, S. E.; Kitsopoulos, T. N.; Neumark, D. M. *J. Chem. Phys.* **1991**, *95*, 8753.
(33) Zhai, H. J.; Liu, S. R.; Li, X.; Wang, L. S. *J. Chem. Phys.* **2001**, *115*, 5170.
(34) Kohno, M.; Suzuki, S.; Shiromaru, H.; Koabyashi, K.; Nagase, S.; Achiba, Y.; Kietzmann, H.; Kessler, B.; Gantefor, G.; Eberhardt, W. *J. Electron. Spectrosc.* **2000**, *112*, 163.
(35) Wang, X. B.; Ding, C. F.; Wang, L. S. *J. Phys. Chem. A* **1997**, *101*, 7699.
(36) Hotop, H.; Lineberger, W. C. *J. Phys. Ref. Data* **1985**, *14*, 731.
(37) Harris, H.; Dance, I. *J. Phys. Chem. A* **2001**, *105*, 3340.
(38) Kittel, C. *Introduction to Solid State Physics*, 2nd ed.; J. Wiley & Sons: New York, 1956.
(39) Baguenard, B.; Pinare, J. C.; Bordas, C.; Broyer, M. *Phys. Rev. A* **2001**, *63*, 23204.
(40) Stairs, J. R.; Davis, K. M.; Peppernick, S. J.; Castleman, A. W., Jr. *J. Chem. Phys.* **2003**, *119*, 7857.